

## Elastic Properties of Glasses

H. He and M. F. Thorpe

*Department of Physics and Astronomy, Michigan State University, East Lansing, Michigan 48824*  
(Received 16 October 1984)

It is believed that covalent glasses can be divided into two classes: those with high average coordination (amorphous solids) and those with low average coordination (polymeric glasses). We present the first conclusive evidence that this division is correct by calculating the elastic properties of random networks with different average coordination  $\langle r \rangle$ . The results show that the elastic constants depend predominantly on  $\langle r \rangle$  and go to zero when  $\langle r \rangle = 2.4$  with an exponent  $f = 1.5 \pm 0.2$ .

PACS numbers: 61.40.Df, 62.20.Dc

The notion of *overconstrained* and *underconstrained* glasses was introduced by Phillips<sup>1</sup> in 1979. This idea was later put on a firm foundation by Thorpe<sup>2</sup> who envisaged a glass consisting of *rigid* and *floppy* regions and a phase transition taking place as the mean coordination  $\langle r \rangle$  is increased and *rigidity percolates* through the network. In this Letter we present results of numerical simulations for the elastic moduli, and for the number of zero-frequency modes  $f$ , of a series of glassy networks. These two quantities couple most directly to the phase transition. Our results show conclusively that there is indeed a phase transition when the network has  $\langle r \rangle = 2.4$  and that both the elastic moduli and  $f$  depend predominantly on  $\langle r \rangle$ . The ideas of Phillips and Thorpe can now be applied to real

covalent glasses with some confidence.

We consider covalent glasses (e.g.,  $\text{Si}_x\text{O}_{1-x}$ ) to be continuous random networks.<sup>3</sup> This model is widely believed to provide an excellent description of many glasses. Some of the results of this Letter would also be applicable to models which use rafts, ribbons, finite clusters, etc.<sup>4</sup>

Consider that a particular random network with  $N$  atoms has been constructed with  $n_r$  atoms having  $r$  bonds, where  $r = 2, 3$ , or  $4$  for covalent networks and

$$\sum_r n_r = N. \quad (1)$$

This network is relaxed into the local equilibrium for the given topology and small vibrations about this equilibrium structure are described by a potential<sup>5</sup>

$$V = \frac{1}{2} \sum_{\langle ij \rangle} \alpha_{ij} [(\mathbf{u}_i - \mathbf{u}_j) \cdot \mathbf{r}_{ij}]^2 + \frac{1}{8} \sum_{\langle ijk \rangle} \beta_{ijk} [(\mathbf{u}_i - \mathbf{u}_j) \cdot \mathbf{r}_{ik} + (\mathbf{u}_i - \mathbf{u}_k) \cdot \mathbf{r}_{ij}]^2, \quad (2)$$

where  $\alpha_{ij}$  is a central force involving nearest neighbors  $(i, j)$  and  $\beta_{ijk}$  is a Keating-type angular force involving pairs of nearest neighbors  $(i, j)$  and  $(i, k)$ . Before describing the results of the simulations it is useful to develop a mean-field theory for the number of zero-frequency modes.<sup>6</sup>

When the coordination of the network is low, there are many ways in which the network can be deformed at no cost in energy because there is no term in the potential (2) that couples directly to the dihedral angles. Deformations are possible in which the bond angles and bond lengths are unchanged. The number of these deformations or *zero-frequency modes* is given by the number of the degrees of freedom ( $3N$ ) minus the number of *constraints*. There is one constraint associated with each bond and  $2r - 3$  constraints associated with the angles at each  $r$ -coordinated atom.<sup>2,7</sup> The fraction  $f$  of zero-frequency modes is given by

$$f = \{3N - \sum_r n_r [r/2 + (2r - 3)]\} / 3N \\ = 2 - \frac{5}{6} \langle r \rangle, \quad (3)$$

where

$$\langle r \rangle = \sum_r r n_r / \sum_r n_r \quad (4)$$

is the mean coordination. It is important in applying (4) that the network contain no dangling bonds. Equation (3) is plotted as the straight line in the inset in Fig. 1. For  $\langle r \rangle = 2$ , which corresponds to isolated noninteracting polymer chains,  $f = \frac{1}{3}$ . As  $\langle r \rangle$  increases (which can be imagined as a crosslinking of the polymer chains to form a network),  $f$  decreases and goes to zero at  $\langle r \rangle = r_p = 2.4$ . As negative values of  $f$  are meaningless, we put  $f = 0$  for  $\langle r \rangle > r_p$  within this mean-field theory.

Similar constraint-counting arguments have been used by Feng, Thorpe, and Garboczi<sup>6</sup> to estimate where  $f$  goes to zero and hence where the phase transition takes place. They find that the mean-field theory is *remarkably* accurate, when compared to direct calculations of both  $f$  and the elastic moduli, in dilute lattices with *central forces only*.

The result,  $r_p = 2.4$ , was obtained by Döhler, Dandoloff, and Bilz<sup>7</sup> and by Thomas<sup>8</sup> using the ideas of Phillips.<sup>1</sup> For  $2 < \langle r \rangle < r_p$ , we have a *polymeric glass* with rigid and floppy regions, but the rigid regions do not percolate. For  $\langle r \rangle > r_p$ , we have an *amorphous solid* in which the rigid regions percolate.<sup>2</sup>

We have performed numerical simulations for both

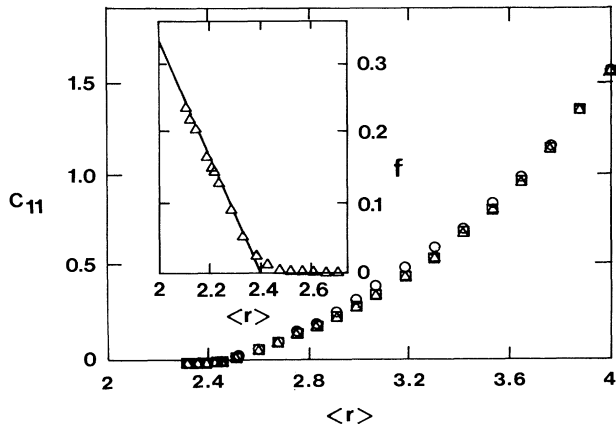


FIG. 1. Elastic modulus  $C_{11}$  with  $\beta/\alpha=0.2$  in units where  $\alpha=4a$  and as a function of the mean coordination  $\langle r \rangle$ . The three symbols are for three different series of random networks. The inset shows the number of zero-frequency modes  $f$  (averaged over three networks) compared to the result of the mean-field theory [Eq. (3)] shown by a straight line.

$f$  and the elastic moduli. It is rather difficult to build large numbers of random networks, with varying coordination, and so we have adopted the following approach which we believe captures the essential physics.

We start with a diamond lattice that has  $\langle r \rangle = 4$  and define a supercell which contains 512 (or 216) atoms. We then randomly remove bonds, maintaining the structure with periodic boundary conditions so that if a bond is removed in one supercell it is removed in all supercells. When a bond is removed, all the  $\alpha$  and  $\beta$  terms associated with it are removed from the potential (2). At first only three-coordinated sites are created, but with enough bonds removed, two-coordinated sites are also created. No dangling bonds are permitted.

In Fig. 2 we show a plot of  $n_3/N$  against  $\langle r \rangle$  for the 512-atom networks. Note that

$$\langle r \rangle = (2n_2 + 3n_3 + 4n_4)/N, \quad (5)$$

where  $N = n_2 + n_3 + n_4$  so there is one free parameter in the process described in the previous paragraph. The triangles and squares in Fig. 2 are "typical" results using different random numbers. In order to test whether the properties of the network depended mainly on  $\langle r \rangle$  and not on other parameters, we deliberately picked one "extreme" configuration with an enhanced number of two-coordinated sites  $n_2$ , thereby depressing  $n_3$  as shown by the circles in Fig. 2. As  $\langle r \rangle$  approaches 2, it became impossible to remove bonds without creating dangling ends, so that we could not explore the region  $\langle r \rangle \leq 2.1$ .

Our calculations for the elastic moduli were done on the 512-atom networks, but the calculations of  $f$  were

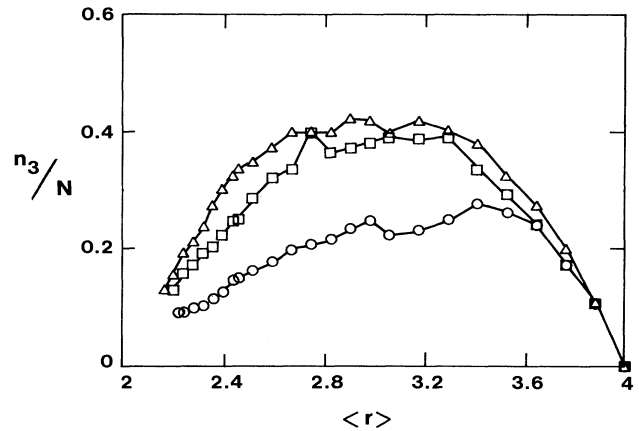


FIG. 2. Fraction of three-coordinated sites  $n_3/N$  as a function of the mean coordination  $\langle r \rangle$ . The three different symbols represent the three different series of random networks as described in the text. The lines are for guidance of the eye only.

done on the 216-atom networks of which we also generated three with statistics similar to those shown in Fig. 2 (i.e., two were "typical" and one was "extreme"). We computed  $f$  for all three classes of network by directly diagonalizing the dynamical matrix formed from the potential (2) and counting the number of zero eigenvalues. There was no significant variation between the three networks and the averaged result is shown as the inset in Fig. 1. The agreement with mean-field theory is very good. The tail around  $r_p = 2.4$  is somewhat larger than in central-force models<sup>6</sup> but is still small. We do not expect  $f$  to be precisely zero at  $r_p$  as floppy regions still exist after the rigid regions have percolated.

We have also computed the elastic moduli of these systems. The three elastic moduli for the diamond lattice are<sup>5</sup>

$$B = \frac{1}{3}(C_{11} + 2C_{12}) = \frac{1}{12a}(3\alpha + \beta), \quad (6)$$

$$C_{11} = \frac{1}{4a}(\alpha + 3\beta), \quad C_{44} = \frac{1}{a} \frac{\alpha\beta}{(\alpha + \beta)},$$

and we choose  $\beta/\alpha = 0.2$  which is a typical value for covalent solids and  $a/\sqrt{3}$  is the nearest-neighbor distance.<sup>9</sup>

The elastic moduli are computed with use of standard techniques.<sup>6,10</sup> The 512-atom supercell is redefined by an external strain  $\epsilon$  and the elastic modulus  $C$  is obtained from the elastic energy  $\frac{1}{2}C\epsilon^2$  after the network has been fully relaxed. This relaxation becomes very difficult for  $\langle r \rangle \leq 2.6$  and we used extrapolation techniques to obtain the behavior at longer times,  $t$ , than could be probed. The long-time behavior seemed to follow  $C(t) = C + D \exp(-\gamma t)$  and we used this to

extract the desired asymptotic elastic modulus  $C$ . Here time refers to the number of steps in the relaxation process.

In Fig. 1 we show the results for  $C_{11}$  (averaged over the  $x$ ,  $y$ , and  $z$  directions) for the three systems. It can be seen that these are all very similar, although the circles lie a little above the other two. From this, and the inset, we see that the elastic properties of the network are determined, essentially entirely, by  $\langle r \rangle$ .<sup>11</sup> This remarkable universal result, implicit in the work of Phillips, has many implications for glasses (e.g., low-temperature specific heat, ultrasonic attenuation) that will undoubtedly be explored in the years to come.

In Fig. 3 we show the three elastic moduli as a function of  $\langle r \rangle$ . It should be noted that both  $B$  and  $C_{44}$  show similar, although slightly larger, variations between the three networks as shown in Fig. 1 for  $C_{11}$ . It can be seen that all the elastic moduli go to zero around  $r_p \approx 2.4$  as predicted by mean-field theory.

We have made log-log plots of the elastic moduli for  $2.4 < \langle r \rangle < 3.2$  and find a slope of  $1.5 \pm 0.2$ . We have also made a least-squares fit to the data in the same range with an exponent of 1.5 and find that

$$\begin{aligned} C_{11} &= 0.69(\alpha/4a)(\langle r \rangle - r_p)^{1.5}, \\ B = C_{44} &= 0.35(\alpha/4a)(\langle r \rangle - r_p)^{1.5}. \end{aligned} \quad (7)$$

We do not claim that the critical exponent is 1.5; merely that the functional form (7) is appropriate over a fairly large range. It does *not* fit the data well at larger values of  $\langle r \rangle$ . In the central-force models,<sup>6</sup> the data were linear over the whole range (corresponding to an exponent of 1) with the possibility of a small "tail" near the phase transition corresponding to the critical region. Similarly here there could very well be

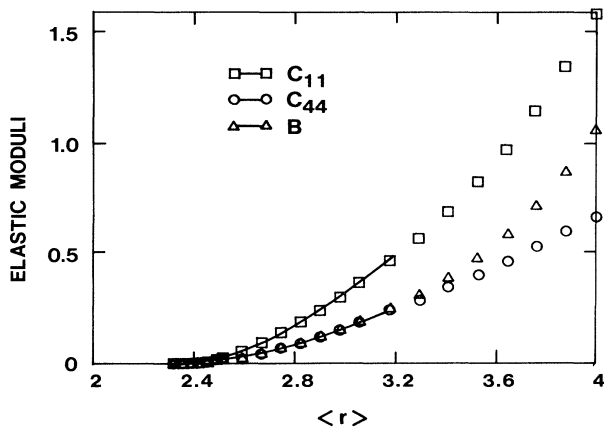


FIG. 3. Elastic moduli averaged over all three networks as a function of the mean coordination  $\langle r \rangle$  for  $\beta/\alpha = 0.2$ . The elastic moduli are in units where  $\alpha = 4a$  and the solid lines are from Eq. (7). The results for  $C_{11}$  and  $C_{44}$  have been averaged over the  $x$ ,  $y$ , and  $z$  directions.

deviations from (7) very close to  $r_p$  in the critical region. We can refer to (7) as the *mean-field behavior*.<sup>12</sup>

Finally we note that the networks are cubic, not isotropic. Initially when  $\langle r \rangle = 4$  and  $\beta/\alpha = 0.2$ , the anisotropy parameter  $A = (2C_{44} - C_{11} + C_{12})/C_{11}$  is 0.33 but has dropped to 0.29 in the region covered by (7), and drops rapidly to 0.10 for  $\langle r \rangle = 2.4$ . Indeed it could very well be going to zero at  $r_p$  but our results are very noisy for  $\langle r \rangle \leq 2.45$  in the critical region.<sup>13</sup> Such an isotropic result would not be unexpected as the system probably consists of long thin rigid regions, near  $r_p$ , that interlace one another and the local geometry becomes unimportant.<sup>14</sup> If we do an average over all the principle directions (100, 110, and 111) with relative weights (6, 12, and 8) we find that

$$\begin{aligned} \langle v_l^2 \rangle / \langle v_t^2 \rangle &= (C_{11} + \frac{17}{39}AC_{11}) / (C_{44} - \frac{17}{78}AC_{11}) \\ &= \begin{cases} 3.3 & \text{for } \langle r \rangle = 4, \\ 2.4 & \text{for } 2.4 < \langle r \rangle < 3.2, \end{cases} \end{aligned} \quad (8)$$

where  $v_l$  is the longitudinal sound velocity and  $v_t$  is the transverse sound velocity.<sup>15</sup>

Before beginning this work we had hoped to find a more pronounced singularity in the elastic moduli at  $r_p$  which would facilitate experimental observation. In real glasses, especially with small  $\langle r \rangle$ , dihedral angle forces, van der Waals forces, etc., are needed to stabilize the structure. These will add a small, weakly  $\langle r \rangle$ -dependent term to the elastic moduli shown in Fig. 3.

The support of the National Science Foundation and the Office of Naval Research is acknowledged. We are also grateful to Colorado State University for the use of their CYBER 205 computer. Numerous discussions with E. Garboczi are gratefully acknowledged.

<sup>1</sup>J. C. Phillips, J. Non-Cryst. Solids **34**, 153 (1979), and **43**, 37 (1981).

<sup>2</sup>M. F. Thorpe, J. Non-Cryst. Solids **57**, 355 (1983).

<sup>3</sup>W. H. Zachariasen, J. Am. Chem. Soc. **54**, 3841 (1932); D. E. Polk, J. Non-Cryst. Solids **5**, 365 (1971).

<sup>4</sup>J. C. Phillips, J. Non-Cryst. Solids **34**, 153 (1979), and Phys. Status Solidi B **101**, 473 (1980).

<sup>5</sup>P. N. Keating, Phys. Rev. **145**, 637 (1966).

<sup>6</sup>S. Feng, M. F. Thorpe, and E. Garboczi, Phys. Rev. B **31**, 276 (1985).

<sup>7</sup>G. H. Döhler, R. Dandoloff, and H. Bilz, J. Non-Cryst. Solids **42**, 87 (1983).

<sup>8</sup>N. Thomas, Ph.D. thesis, University of Cambridge, 1978 (unpublished).

<sup>9</sup>M. F. Thorpe, in *Vibrational Spectroscopy of Molecular Liquids and Solids*, edited by S. Bratos and R. M. Pick (Plenum, New York, 1980), p. 341.

<sup>10</sup>S. Feng and P. N. Sen, Phys. Rev. Lett. **52**, 216 (1984).

<sup>11</sup>The initial slope of  $C_{11}$  in Fig. 1, for  $\langle r \rangle$  near 4, is determined by a single missing band and so is the same for all samples. The constraint-counting argument (which is verified numerically in the inset in Fig. 1) shows that  $C_{11}$  goes to zero at  $\langle r \rangle = r_p = 2.4$ . As  $C_{11}$  is expected to be a smooth function of  $\langle r \rangle$ , it is not surprising that  $C_{11}$  is determined by  $\langle r \rangle$ . Similar arguments hold for all the elastic moduli.

<sup>12</sup>J. C. Phillips and M. F. Thorpe, *Solid State Commun.* **53**, 699 (1985).

<sup>13</sup>H. He and M. F. Thorpe, unpublished.

<sup>14</sup>A similar picture has been developed around the "node-

link model" by Y. Kantor and J. Webman, *Phys. Rev. Lett.* **52**, 1891 (1984).

<sup>15</sup>Universal values for  $v_l/v_t$  at the phase transition have been proposed for isotropic elastic systems by D. J. Bergman and Y. Kantor, *Phys. Rev. Lett.* **53**, 511 (1984); D. J. Bergman *Phys. Rev. B* **31**, 1696 (1985); M. F. Thorpe and P. Sen, unpublished. These systems are simpler as the phase transition takes place when the system breaks up into separate pieces (i.e., ordinary geometrical percolation). By universal we mean independent of the material parameters (e.g.,  $\beta/\alpha$ ).